This is an *Accepted Manuscript*, which has been through the Royal Society of Chemistry peer review process and has been accepted for publication.

Accepted Manuscripts are published online shortly after acceptance, before technical editing, formatting and proof reading. Using this free service, authors can make their results available to the community, in citable form, before we publish the edited article. We will replace this *Accepted Manuscript* with the edited and formatted *Advance Article* as soon as it is available.

You can find more information about *Accepted Manuscripts* in the **Information for Authors**.

Please note that technical editing may introduce minor changes to the text and/or graphics, which may alter content. The journal's standard **Terms & Conditions** and the **Ethical guidelines** still apply. In no event shall the Royal Society of Chemistry be held responsible for any errors or omissions in this *Accepted Manuscript* or any consequences arising from the use of any information it contains.

Chemical Communications

COMMUNICATION

Formation of N_3^- during interaction of NO with reduced ceria

Mihail Y. Mihaylov,[a] Elena Z. Ivanova,[a] Hristiyan A. Aleksandrov,[b] Petko St. Petkov,[b] Georgi N. Vayssilov,[b],* and Konstantin I. Hadjiivanov[a],*

We show that the first stages of interaction between NO and reduced ceria comprise the formation of azides, N_3^-, with simultaneous oxidation of Ce^{3+} to Ce^{4+}. This finding impose revision of some current views of catalytic NO conversion and may contribute to design new $deNO_x$ materials and processes.

The need for more effective $deNO_x$ technologies has provoked continuously increasing interest in nitrogen monoxide interaction with solid surfaces. There are different routes for catalytic conversion of NO to N_2 and most of the catalysts contain transitional metal cations. Normally, these cations change their oxidation states in the course of the catalytic reaction. Therefore, for successful design of effective $deNO_x$ catalysts, it is important to know the nature of the species formed during NO interaction with reduced and oxidised materials.

Ceria is a component in many catalysts for NO_x conversion, e.g., three-way,[1] storage reduction,[2,3] selective catalytic reduction[4,5] and soot oxidation (by NO_x) catalysts.[6] In addition, the emerging biological application of ceria nanoparticles is based on their ability to fix free radicals, such as NO, under physiologically relevant conditions.[7,8]

Many studies deal with the nature of the species formed during interaction of NO_x with ceria[5,9-20] and ceria-containing systems.[4,9,21-28] Most of them have used infrared spectroscopy because this technique provides valuable information on the nature of the surface species. Following the pioneering study of Niwa et al.[10] many authors[4,11,14-29] reported the formation of NO^-, cis- and trans-hyponitrites, nitrites, and/or nitrates. However, although the $deNO_x$ activity of ceria was found to correlate with the number of oxygen vacancies,[5] little attention has been paid to the surface species and intermediates formed on reduced samples.[5,13,15]

Here we report the results of a careful study of the nature of surface species formed during NO interaction with reduced ceria. We have used mainly FTIR spectroscopy of adsorbed ^{14}NO, ^{15}NO, and $^{14}NO + ^{15}NO$ isotopic mixtures and state-of-the-art density functional (DF) calculations. To distinguish different species and to follow the order of their formation, successive adsorption of small NO doses was performed. The reduction degree of ceria was monitored by the $^2F_{5/2} \rightarrow {}^2F_{7/2}$ electronic

transition band of Ce^{3+} at 2118 cm^{-1}.[30] The adsorption of ^{15}NO provided information on the nature of the bonds formed because the $^{15}N/^{14}N$ isotopic shift factors for N–N and N–O bonds markedly differ.[31] With this approach, we provide spectral evidence of the formation of surface azide species, N_3^- during NO adsorption on reduced ceria. These species are detected for the first time after adsorption of NO on solids. The observations impose a revision of some current opinions on the mechanisms of catalytic NO conversion.

Two samples of different origin were investigated to differentiate between the properties typical of the oxide and the morphology effects. The $CeO_2(A)$ sample was supplied by Rhodia (France) and had a specific surface area of 170 m^2g^{-1}. The $CeO_2(B)$ sample had a similar specific surface area (173 m^2g^{-1}) and was supplied from Daiichi Sankyo (Japan). The IR investigations were conducted using a Nicolet 6700 spectrometer equipped with a MCT detector at a spectral resolution of 2 cm^{-1}. Self-supporting pellets were prepared by pressing the sample powder at 100 kPa, and the pellets were directly analysed in the IR cell. The latter was connected to a vacuum apparatus with a residual pressure of 10^{-4} Pa. Prior to the experiment the samples were activated by heating at 773 K for 1 h in oxygen (20 kPa) and evacuation for 1 h at the same temperature. Then, the samples were reduced with hydrogen (150 kPa) for 60 min at 773 K, followed by 1 h evacuation at the same temperature. These procedures were repeated three times in order to minimize the amount of residual carbonates that are always present on activated ceria. Nitrogen monoxide (> 99.5 % purity), O_2 (> 99.999 %) and H_2 (> 99.999 %) were purchased from Messer. ^{15}NO (> 99 % isotopic purity) was supplied by Isotec Inc. and was diluted in He (molar ratio of NO:He = 1:10). NO was additionally purified by fraction distillation. Oxygen and hydrogen were additionally purified by passing through a liquid nitrogen trap.

The calculations are performed using a periodic plane-wave DFT method with PW91 exchange-correlation functional of a generalised-gradient (GGA) type as implemented in the VASP program[32]. The ceria is described within the so-called GGA+U approach, in which on-site Coulombic interaction with U = 4 eV is included.[32,33] The kinetic energy cut-off is 415 eV. Ceria is modelled as a stoichiometric nanoparticle $Ce_{21}O_{42}$ with a

diameter of 1.0 nm and it exhibits the crystallinity of the fluorite structure of CeO$_2$ that was previously used for the modelling of nanostructured ceria systems.[32-34] The space between neighbouring slab images is 1.0 nm. The CeO$_2$(111) surfaces are modelled with a slab Ce$_{54}$O$_{108}$ of three CeO$_2$ (eighteen atomic) layers and a 3×6 surface cell. Complete geometry optimisation has been performed for the nanoparticle and slab models. The stability of the formed species was evaluated by the adsorption energy (Table 1), with respect to corresponding number of NO molecules and reduced ceria models. The harmonic vibrational frequencies of the adsorbed species are calculated numerically and scaled by a factor of 0.952 for the N–N mode. The scaling factors are determined from the calculated and experimental frequencies in the gas phase of N$_2$O, N$_2$, and HN$_3$.

The background IR spectra of the reduced ceria samples are consistent with previously published results (see Fig. S1 from ESI)[5,30]. In particular, a band at 2118 cm^{-1} due to the Ce^{3+} electronic transition was observed. The FTIR spectra of small doses of NO and ^{15}NO successively adsorbed on reduced CeO$_2$ samples show only two groups of IR bands that are sensitive to the ^{14}N/^{15}N substitution. Their maxima are around 2041 and at 989 cm^{-1}, respectively (see Fig. S2 from the ESI). The relative intensity of the bands is markedly different for the two samples (see Fig. S3 from ESI) which indicates that (i) they belong to different species and (ii) these species are formed with participation of different surface sites. With the development of the bands under consideration ceria is oxidised as evidenced by the parallel disappearance of the Ce^{3+} electronic transition at 2118 cm^{-1} (see the negative bands in Fig 1). Other bands sensitive to the isotopic substitution are formed only at higher coverage and will be not discussed here.

A reliable criterion for distinguishing different types of bonds is the isotopic shift factor. The theoretical isotopic shift factors are 1.035 for $\nu(^{14}N-^{14}N)/\nu(^{15}N-^{15}N)$ and 1.018 for $\nu(^{14}N-O)/\nu(^{15}N-O)$.[31] The observed isotopic shift factor for the band at 989 cm^{-1} is 1.019 which implies it is due to N-O stretching modes. Bands in this region, registered after NO adsorption of ceria-containing systems, have already been reported and assigned to *cis*-hyponitrite species.[11,14] Here we will not concentrate on these bands.

In contrast, the band at 2044-2041 cm^{-1} has never been reported earlier with ceria and ceria-based systems. No concomitant bands were observed. The isotopic shift factor of the 2044-2041 band is 1.034, implying that it characterises nitrogen–nitrogen bond(s). Upon adsorption of the ^{14}NO + ^{15}NO isotopic mixture (1 : 1 molar ratio), the band appears as a sextet (see panels C and D in Fig. 1) indicating that the respective species contains three nitrogen atoms. The intensities of the bands in the sextet follow a statistical distribution consistent with highly symmetric species with two equivalent and one different nitrogen atoms (for more details see Fig. S4 from ESI and the corresponding text). Based on these result, the 2044-2042 cm^{-1} band is assigned to the antisymmetric ^{14}N-^{14}N stretching modes of azide species, ^{14}N$_3^-$ (16-electon structure). Because of the high symmetry, the respective ν_s stretching mode is IR silent. This assignment is consistent with the published data on the spectral performance of azides.[35,36] The formation of surface azides has been suggested after NH$_3$ oxidative adsorption on several catalysts[37,38] but their structure was not proven by isotopic studies. Here we report for the first time the formation of N$_3^-$ as a result of NO reductive adsorption on solid surfaces, and the assignment is confirmed by isotopic experiments.

The above findings are fully supported by the DFT
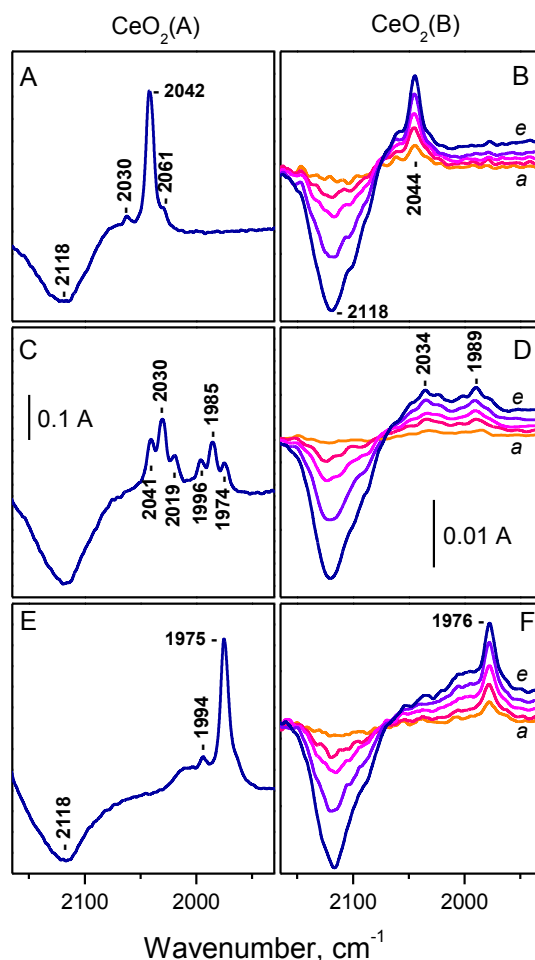
Fig. 1. Experimental spectra of the azide, N$_3^-$, species on ceria: Background corrected FTIR spectra registered after adsorption of ^{14}NO (A, B), ^{14}NO + ^{15}NO (C, D) and ^{15}NO (E, F) on reduced CeO$_2$ samples. Sample CeO$_2$(A) (A, C, E), sample CeO$_2$(B) (B, D, F). The spectra for the CeO$_2$(A) sample correspond to the adsorption of 150 μmol NO g^{-1} CeO$_2$. The spectra for the CeO$_2$(B) sample correspond to successive adsorption of small NO doses [2 (a), 4 (b), 6 (c), 9 (d) and 12 (e) doses, each of 7 μmol g^{-1}]. The Y-axes scales are equal for each sample.

calculations. Different azide species were modelled on ceria nanoparticles, and two of them (Fig. 2, panels A, B) feature the high symmetry indicated by the experiment. The vibration frequency of those species, 2033 cm^{-1}, is close to the experimentally observed values (see Table 1). Moreover, the calculated frequencies of the species with all possible arrangements of ^{14}N and ^{15}N isotopes in the N$_3^-$ moiety fit excellently to the experimental values (see Table 1). The symmetric N$_3^-$ structures are formed at the edges of the ceria nanoparticle. Similar species were also modelled on the CeO$_2$ (111) surface (Fig. 2, panel C). The vibrational frequency of the latter species was by 30 cm^{-1} lower than that on the nanoparticles, but their simulated isotopic shifts also fit well to the sextet arrangement observed experimentally (Table 1). Therefore, the most favourable location of N$_3^-$ moities is at crystal edges or facets. A careful inspection of the spectra presented in Fig. 1A shows weak satellite bands at 2061 and 2030 cm^{-1}, suggesting some heterogeneity and different locations of N$_3^-$.
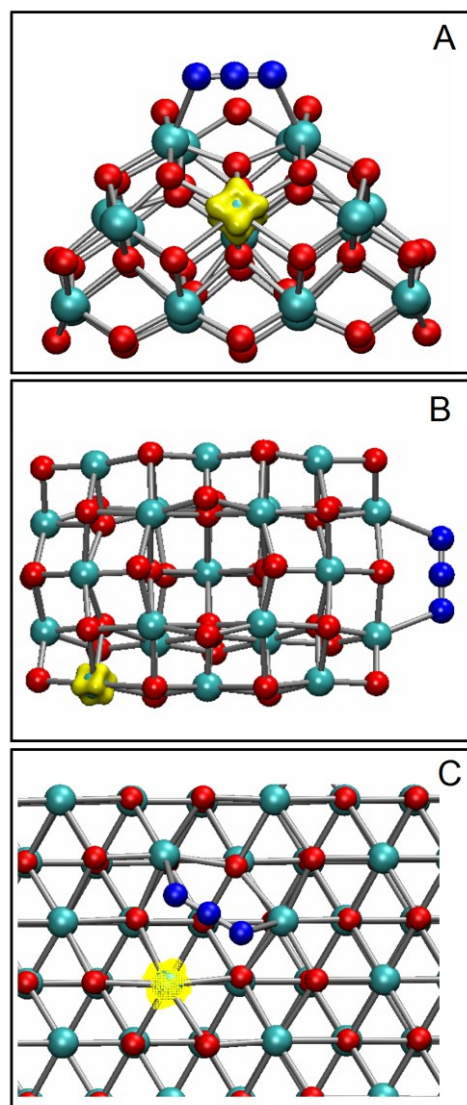
Fig. 2. Azide structures obtained with DFT modelling: structures $[N_3^-]$-a (A) and $[N_3^-]$-b (B) on the nanoparticle and $[N_3^-]$-c (C) on CeO_2(111) surface (colour coding: dark blue - nitrogen, red – oxygen, dark cyan - cerium, yellow – unpaired electron density).

Table 1. Calculated NO adsorption energy during the formation of N_3^- species on ceria (species a - e), E_{ads}(NO) in eV, and characteristic experimental and calculated vibrational frequencies and isotopic shifts[a] of the species in cm^{-1}.

Species	E_{ads}(NO)	v, cm^{-1}	Shifts for $^{14}NO/^{15}NO$ mixture[a]							
			lll	*lli*	*ill*	*lil*	*ili*	*iil*	*lii*	*lll*
$[N_3^-]$-exp	-	2044	0	-11	-11	-22	-45	-56	-56	-67
$[N_3^-]$-a	-7.39	2033	0	-10	-10	-22	-46	-57	-57	-69
$[N_3^-]$-b	-7.75	2033	0	-10	-10	-22	-46	-57	-57	-69
$[N_3^-]$-c	-10.91	2002	0	-11	-11	-22	-45	-56	-56	-68
$[N_3^-]$-d	-7.11	2062	0	-14	-7	-45	-23	-52	-60	-69
$[N_3^-]$-e	-6.66	2021	0	-20	-5	-45	-25	-49	-66	-70

[a] The different nitrogen isotops in N_3^- species are denoted as "*l*" for ^{14}N and "*i*" for ^{15}N, for example *ill* correspons to $^{15}N^{14}N^{14}N$.

Stoichiometrically, the process leading to the formation of N_3^- involves oxidation of seven Ce^{3+} ions to Ce^{4+} by three NO molecules with the simultaneous filling of three oxygen vacancies. Due to the latter fact, as well as to the creation of two N–N bonds, the formation of azide anions is a highly exothermic process, with a calculated reaction energy Er = -7.39 to -7.75 eV (Table 1). On CeO_2 (111) surface the reaction energy, Er = -10.91 eV, is even higher since the oxygen vacancy formation energy is higher on the surface.[32,33] Indeed, the energy for filling three oxygen vacancies on ceria nanoparticle is calculated -5.82 eV, while on CeO_2 (111) surface this energy is -8.94 eV.

The azide ion is isoelectronic with NCO^-. It is well known that surface isocyanates are important intermediates in the selective catalytic reduction of NOx with hydrocarbons.[38-40] The NCO^- species are thermally stable and hardly interact with NO or O_2 alone but easily disappear in mixtures of the two gases with the formation of dinitrogen.[38,39] We found that the surface azides demonstrated very similar properties (Fig S5). They decompose above 573 K and are stable in the presence of NO (at low equilibrium pressure) or O_2 alone in the gas phase at 298 K. However, the addition of a small amount of O_2 to NO leads to a rapid disappearance of the azides (See Fig. S3 from the ESI) and simultaneous production of nitrito- and nitrato-species was detected. Consumption of azides was also established at high NO equilibrium pressures because at these conditions some NO_2 is formed. Fig. S5 shows that no intermediate species with N-N bond are formed during interaction of azides with NO + O_2. This observation indicates that dinitrogen is evolved during interaction between N_3^- and NO_2, likely according to a mechanism similar to that of the interaction between NCO^- and NO_2.

Several of the mechanisms proposed for the formation of dinitrogen during NOx catalytic reduction involve coupling of two nitrogen-containing moieties, one with nitrogen in positive, and the other, in negative formal oxidation state. For instance, it is believed that intermediated in the reduction of NO_x with NH_3 are NH_4NO_2 or NH_4NO_3 species.[41] Interaction of amines and NO^+ is suggested to lead to dinitrogen via formation of diazonium salts.[39] As already noted, coupling of NCO^- and NO_2 is proposed for the reduction of NO_X with hydrocarbons. Here we identified another species for coupling with a NO_X molecule, i.e. azide ion, where the formal nitrogen oxidation state is -1/3. Thus, it seems that, with ceria containing storage reduction catalysts, N_3^- is formed when NO interacts with the reduced surface. In the next step, N_3^- interacts with NO_2 to produce dinitrogen.

Conclusions

We have shown that interaction of NO with reduced surfaces can lead to its deep reduction to N_3^- species where the formal nitrogen oxidation state is -1/3. Evidently, the surface azide species are among the intermediates in the conversion of NO on ceria based storage-reduction catalysts and are likely formed during other deNOx adsorption and catalytic processes.

Notes and references

[a] Institute of General and Inorganic Chemistry, Bulgarian Academy of Sciences, Sofia 1113, Bulgaria. Fax: 00 3592 8705024; Tel: 00 3592 979 3598; E-mail: kih@svr.igic.bas.bg

[b] Faculty of Chemistry and Pharmacy, University of Sofia, 1126 Sofia, Bulgaria; E-mail: gnv@chem.uni-sofia.bg

1 A. Trovarelli, *Catal. Rev. - Sci. Eng.*, 1996, **38**, 439-520.

2 Z. Say, E. I. Vovk, V. I. Bukhtiyarov and E. Ozensoy, *Appl. Catal. B*, 2013, **142–143**, 89–100.

3 A. Filtschew, D. Stranz and C. Hess, *Phys. Chem. Chem. Phys.*, 2013, **15**, 9066–9069.

4 G. Qi, R. T. Yang and R. Chang, *Appl. Catal. B*, 2004, **51**, 93–106.

5 M. Daturi, N. Bion, J. Saussey, J.-C. Lavalley, C. Hedouin, T. Seguelong and G. Blanchard, *Phys. Chem. Chem. Phys.*, 2001, **3**, 252–255.

6 N. Zouaoui, M. Issa, D. Kehrli and M. Jeguirim, *Catal. Today*, 2012, **189**, 65−69.

7 E. G. Heckert, A. S. Karakoti, S. Seal and W. T. Self, *Biomaterials* 2008, **29**, 2705–2709.

8 J. M. Dowding, T. Dosani, A. Kumar, S. Seal and W. T. Self, *Chem Commun.* 2012, **48**, 4896–4898.

9 J. Paier, A. Penschke and J. Sauer, *Chem. Rev.*, 2013, **113**, 3949-3985.

10 M. Niwa, Y. Furukawa and Y. J. Murakami, *J. Colloid Interface Sci.*, 1982, **86**, 260−265.

11 A. Martínez-Arias, J. Soria, J. C. Conesa, X. L. Seoane, A. Arcoya and R. Cataluña, *J. Chem. Soc. Faraday Trans.*, 1995, **91**, 1679–1687.

12 B. Azambre, I. Atribak, A. Bueno-López and A. García-García, *J. Phys. Chem. C*, 2010, **114**, 13300–13312.

13 S. H. Overbury, D. R. Mullins, D. R. Huntley and Lj. Kundakovic, *J. Catal.*, 1999, **186**, 296−309.

14 S. Philipp, A. Drochner, J. Kunert, H. Vogel, J. Theis and E. S. Lox, *Top. Catal.*, 2004, **30/31**, 235–238.

15 L. Zhang, J. Pirce, V. Leung, D. Wang and W. S. Epling, *J. Phys. Chem. C*, 2013, **117**, 8282–8289.

16 S. Yang, Y. Guo, H. Chang, L. Ma, Y. Peng, Z. Qu, N. Yan, C. Wang and J. Li, *Appl. Catal. B*, 2013, **136–137**, 19–28.

17 A. N. Il'ichev, M. D. Shibanova, A. A. Ukharskii, A. M. Kulizade and V. N. Korchak, *Kinet. Catal.*, 2005, **46**, 387–395.

18 M. O. Symalla, A. Drochner, H. Vogel, S. Philipp, U. Göbel and W. Müller, *Top. Catal.*, 2007, **42–43**, 199–202.

19 M. Haneda, T. Morita, Y. Nagao, Y. Kintaichi and H. Hamada, *Phys. Chem. Chem. Phys.*, 2001, **3**, 4696–4700.

20 Y. Chen, J. Wang, Z. Yan, L. Liu, Z. Zhang and X. Wang, *Catal. Sci. & Technol.*, 2015, in press, DOI: 10.1039/C4CY01577K.

21 L. Xu, X.-S. Li, M. Crocker, Z. S. Zhang, A. M. Zhu and C. Shi, *J. Mol. Catal. A*, 2013, **378**, 82–90.

22 Y. Peng, C. Liu, X. Zhang and J. Li, *Appl. Catal. B*, 2013, **140–141**, 276–282.

23 L. Wang, R. Ran, X. Wu, M. Li and D. Weng, *J. Rare Earths*, 2013, **31**, 1074–1080.

24 N. Drenchev, I. Spassova, E. Ivanova, M. Khristova and K. Hadjiivanov, *Appl. Catal. B*, 2013, **138–139**, 362–372.

25 R. Zhang, Q. Zhong, W. Zhao, L. Yu and H. Qu, *Appl. Surf. Sci.*, 2014, **289**, 237–244.

26 Z. M. El-Bahy, *Modern Res. Catal.*, 2013, **2**, 136–147.

27 B. Azambre, L. Zenboury, A. Koch and J. V. Weber, *J. Phys. Chem. C*, 2009, **113**, 13287–13299.

28 M. Konsolakis, *Chem. Eng. J.*, 2012, **183**, 550–551.

29 J. Szanyi and J. H. Kwak, *Chem. Commun.*, 2014, **50**, 14998–15001.

30 C. Binet, A. Badri and J.-C. Lavalley, *J. Phys. Chem.*, 1994, **98**, 6392–6398.

31 K. Hadjiivanov, in Ordered Porous Solids - Recent Advances and Prospects, eds. V. Valtchev, S. Mintova, M. Tsapatis, Elsevier, Amsterdam, 2008; pp. 263–281.

32 G. N. Vayssilov, Y. Lykhach, A. Migani, T. Staudt, G. P. Petrova, N. Tsud, T. Skála, A. Bruix, F. Illas, K. C. Prince, V. Matolín, K. M. Neyman and J. Libuda, *Nature Mater.*, 2011, **10**, 310–315.

33 A. Migani, G. N. Vayssilov, S. T. Bromley, F. Illas and K. M. Neyman, *J. Mater. Chem.*, 2010, **20**, 10535–10546.

34 G. N. Vayssilov, M. Mihaylov, P. St. Petkov, K. I. Hadjiivanov and K. M. Neyman, *J. Phys. Chem. C*, 2011, **115**, 23435–23454.

35 M. G. Samant, R. Viswanathan, H. Seki, P. S. Bagus, C. J. Nelin and M. R. Philpott, *J. Chem. Phys.*, 1988, **89**, 583–589.

36 Q. Zhong, D. A. Steinhurst, E. E. Carpenter and J. C.Owrutsky, *Langmuir*, 2002, **18**, 7401–7408.

37 J. Kritzenberger, J. Jobson, A. Wokaun and A. Baiker, *Catal. Lett.,* 1990, **5**, 73–80.

38 G. Ramis, L. Yi and G. Busca, *Catal. Today*, 1996, **28**, 373–380.

39 E. Joubert, T. Bertin, J.C. Menezo and J. Barbier, *Appl. Catal. B*, 1999, **23**, L83–L87.

TOC Entry

The first stages of interaction between NO and reduced ceria comprise the formation of azides, N_3^-, with simultaneous oxidation of Ce^{3+} to Ce^{4+}.

ChemComm Accepted Manuscript